CFD RESEARCH FOR AIR-TO-AIR MISSILE WITH LATERAL JET CONTROL

Dechuan Sun[1], Xiaohong Jia[2], Xiaogeng Liang[2]
1. College of Astronautics, Northwestern Polytechnical University, Xi'an 710072, China
2. Luoyang Opto-Electro Technology Development Center, Luoyang 471009, China

Abstract

A WENO scheme was used to calculate the flowfield around air-to-air missile (AAM) with lateral jet control. The difference between air jet and hot gas jet, the effect of fins, and the influence of double jets were studied. The results are useful for the application of lateral jet control used in AAM.

1 Introduction

Generally, lateral gaseous jet is used in control of high altitude interceptor or flight vehicle in space, such as KKV, to provide enough lateral force. For higher altitude or in space, atmosphere is so thin that the interaction between jet and atmosphere can be neglected, so the control force produced by the lateral jet is nearly equal to its thrust.

Recently, lateral jet was considered to be used in lower altitude flight vehicle because of its characteristic of quickly responsibility. Because of flying in thicker atmosphere, for air-to-air missile control, there are strong interaction between jets and their environment. It results in boundary layer separation, shock waves, and vortices, which are schematically shown in Fig. 1. This complex interaction will make control force deviate from the jet thrust.

Another problem is that for AAM, solid gas generator or small solid rocket motors were often used to produce thrust. While in CFD research, this hot lateral jet was always considered as air. In this paper, a one-dimensional chemical equilibrium method was used to determine the boundary condition at jet orifice to compare the difference of hot combustion gas and air.
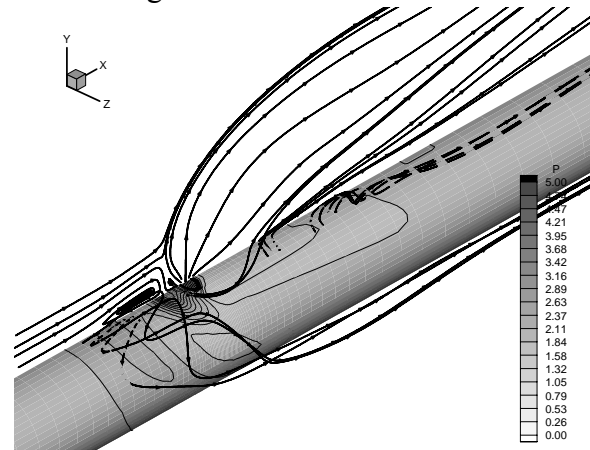

Fig. 1. Main vortexes around the Air-to-Air missile

2 Numerical Method

2.1 Governing Equations

The Favre-averaged N-S equations and low Reynolds k-ε turbulent model are used.

$$\frac{\partial U}{\partial t} + \frac{\partial E}{\partial x} + \frac{\partial F}{\partial y} + \frac{\partial G}{\partial z} = \mathrm{Re}_D^{-1}\left(\frac{\partial E_v}{\partial x} + \frac{\partial F_v}{\partial y} + \frac{\partial G_v}{\partial z}\right) \quad (1)$$

$$p = (\gamma - 1)\left(e - \rho\frac{u^2 + v^2 + w^2}{2} - \rho k\right) \quad (2)$$

$$\mathrm{Re}_D = \frac{\rho_\infty a_\infty D}{\mu_\infty} \quad (3)$$

Where D is the missile diameter and ∞ means the freestream. In the equations, all the variables

were dimensionless. Detail information about the governing equations and the turbulent model can be found in reference 1.

2.2 Spatial discretization

Because of the complexity of the interaction flowfield, higher order difference method should be used. The semidiscrete form of Eq.(1) can be written as

$$\frac{\partial U}{\partial t} = -\left[(E - E_v)_{i+1/2,j,k} - (E - E_v)_{i-1/2,j,k}\right] \\ -\left[(F - F_v)_{i,j+1/2,k} - (F - F_v)_{i,j-1/2,k}\right] \\ -\left[(G - G_v)_{i,j,k+1/2} - (G - G_v)_{i,j,k-1/2}\right] \quad (4)$$

The spatial differencing of numerical fluxes adopts third-order accurate weight essentially non-oscillatory (WENO) scheme of Jiang and Shu [2] for the inviscid convective fluxes and fourth order central differencing for the viscous fluxes.

By adoping WENO schemes, we split the physical fluxes (say, $\hat{F}$) locally into positive and negative part as

$$\hat{F}(\hat{U}) = \hat{F}^+(\hat{U}) + \hat{F}^-(\hat{U}) \quad (5)$$

Where $\partial \hat{F}^+ / \partial \hat{U} \geq 0$, $\partial \hat{F}^- / \partial \hat{U} \leq 0$. Here, the local Lax-Friedrichs flux splitting method is used.

$$\hat{F}^\pm(\hat{U}) = \frac{1}{2}\left(\hat{F}(\hat{U}) \pm |\Lambda|\hat{U}\right) \quad (6)$$

Where $|\Lambda| = diag\left(|\lambda_1|, |\lambda_2|, |\lambda_3|, |\lambda_4|, |\lambda_5|\right)$, and λ_1 , λ_2 , λ_3 , λ_4 , λ_5 are the local eigenvalues.

For one dimensional scalar conservation laws,

$$u_t + f(u)_x = 0 \quad (7)$$

Let us discreticize the space into uniform intervals and denote $x_j = j\Delta x$. The spatial operator of the WENO schemes, which approximates $-f(u)_x$ at x_j , will take the conservative form

$$L = -\frac{1}{\Delta x}\left(\tilde{f}_{j+1/2} - \tilde{f}_{j-1/2}\right) \quad (8)$$

Where $\tilde{f}_{j+1/2}$ and $\tilde{f}_{j-1/2}$ are numerical fluxes. Designate $\tilde{f}_{j+1/2}^+$ and $\tilde{f}_{j+1/2}^-$ respectively the positive and negative parts of numerical flux $\tilde{f}_{j+1/2}$, we have

$$\tilde{f}_{j+1/2} = \tilde{f}_{j+1/2}^+ + \tilde{f}_{j+1/2}^- \quad (9)$$

Here we only describe how to compute $\tilde{f}_{j+1/2}^+$ on the basis of WENO (third-order). $\tilde{f}_{j+1/2}^-$ can be written symmetrically

$$\tilde{f}_{j+1/2}^+ = \omega_0^+\left(\frac{1}{2}f_{j-1}^+ + \frac{1}{2}f_j^+\right) + \omega_1^+\left(\frac{3}{2}f_j^+ - \frac{1}{2}f_{j+1}^+\right)$$

where

$$\omega_k^+ = \frac{\alpha_k^+}{\alpha_0^+ + \alpha_1^+}, \quad k = 0,1$$

$$\alpha_0^+ = \frac{2}{3}\left(\varepsilon + IS_0^+\right)^{-2}, \quad \alpha_1^+ = \frac{1}{3}\left(\varepsilon + IS_1^+\right)^{-2}$$

and

$$IS_0^+ = \left(f_{j-1}^+ - f_j^+\right)^2$$
$$IS_1^+ = \left(f_j^+ - f_{j+1}^+\right)^2$$

2.3 Time discretization

The time discretization of WENO schemes can be implemented by third-order Runge-Kutta method [2]. To solve the ordinary differential equation

$$\frac{du}{dt} = L(u), \quad (10)$$

where $L(u)$ is a discretization of the spatial operator. The third order Runge-Kutta scheme is

$$u^{(1)} = u^n + \Delta t L\left(u^n\right)$$

$$u^{(2)} = \frac{3}{4}u^n + \frac{1}{4}u^{(1)} + \frac{1}{4}\Delta t L\left(u^{(1)}\right) \quad (11)$$

$$u^{n+1} = \frac{1}{3}u^n + \frac{2}{3}u^{(2)} + \frac{2}{3}\Delta t L\left(u^{(2)}\right)$$

3 Boundary Condition at Jet Orifice

Generally, the flow at the jet orifice is always supersonic, and the parameters are controlled by the nozzle area ratio. For small solid rocket motor, angle of divergence and area ratio are all small, so one dimensional calculation can provide enough decision. The method of minimum Gibbs energy often used in rocket performance prediction was used to calculate the flow parameters and gas composition at nozzle exit.

A typical gas composition produced by solid rocket motor at nozzle exit is as follows:

Table 1: composition of gas at nozzle exit

species	Mass fraction	Mole fraction
CO	0.413705	0.282944
CO2	0.037687	0.016405
HCL	0.281723	0.14802
H2	0.037323	0.354679
H2O	0.107943	0.114783
N2	0.121619	0.083169

It is quite different with air. The average molecular weight is 19.39. Capacity of heat is 1813J/kg-K and gas constant is about 430J/kg-K. There are two kinds of methods to simulate the flow field. One is that considering the chemical composition of the hot gas. In this way, we assumed that no chemical reaction occurs between species because of quickly expand, and only mass and heat transfer were considered. The other way is that assuming all the gas in flow field is air. And in this method, we should keep same moment and same pressure at the nozzle exit.

4 Difference between air jet and hot gas jet

The calculation condition is as follows:
  Angle of attack = 0,
  Mach number of freestream =7.0,
  Height = 20 km.

Figure 2 gives the mach number distribution at symmetrical plane. The upper is the result of air jet and the lower is that of gas jet. They are nearly same except the domain of close to the wall.
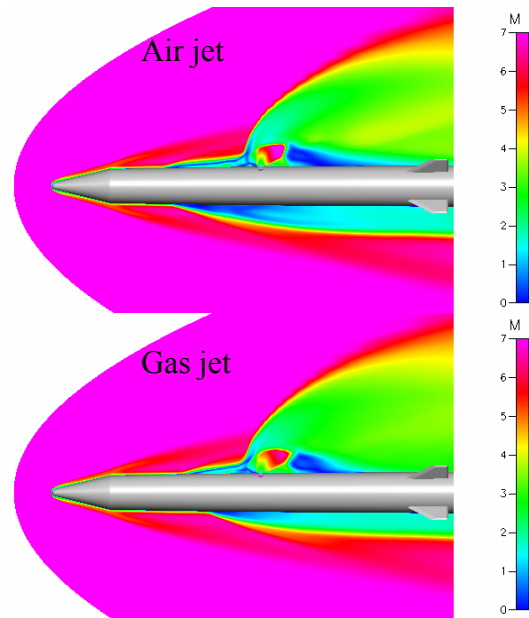

Fig. 2. Mach number distribution at symmetrical plane
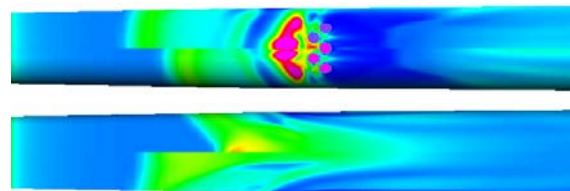

Fig. 3. Comparison of wall pressure between air jet and hot gas jet (inner is gas jet result, outer is air jet result)

Figure 3 shows the difference of wall pressure between air jet and hot gas jet. For convenient, the results are composed to one figure. The outer is air jet result and the inner is hot gas jet. It is apparent that the separation zone of air jet is larger than that of gas jet, especially in upstream of the jet.

By integration of the wall pressure, the amplification factors were obtained. They are 1.02 in case of gas jet and 1.01 in case of air jet. The results are nearly same because of two factors. One is that at 20km high, atmosphere is so thin that the interaction can only influence lateral force finitely. The other is that jet moment and pressure at nozzle exit are main influence factors. To keep same moment and pressure intend to get same results.

In fact, moment and pressure at jet exit are the key factors in transverse supersonic flow. The difference between air jet and gas jet is very little. To save calculation time, the air jet assumption is accurate enough.

5 Effect of fins

For slender body, the influence domain of transverse jet can easily extend around the body. But for missile with long fins, the result will be different. Figure 4 shows a missile with four fins around the body. And there are four lateral jets located at the middle of fins.
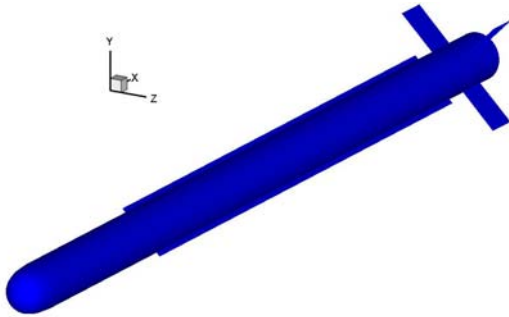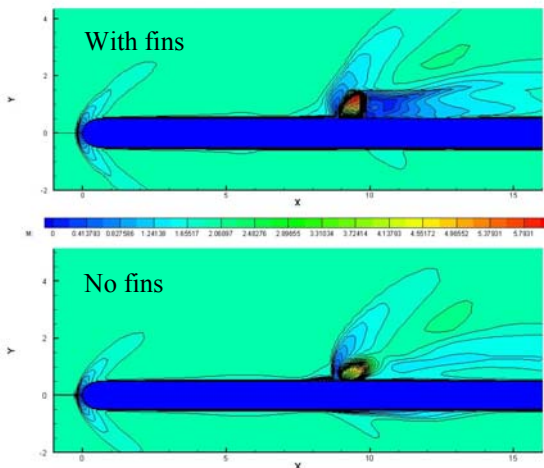

Fig. 4. Schematic of missile with fin

Fig. 5. Comparison of mach number at symmetrical plane

A comparison was given for missile with and without fins under the condition of H=6km, M=2.0, and angle of attack is zero.
Figure 5 shows the difference of Mach number at symmetrical plane. Obviously, fins have great effect on the result. The barrel shock wave is more up-right and the lower pressure zone is larger than those of no fins.
Figure 6 compares the wall pressure distribution. For the case of with fins, the high pressure zone upstream of the jet is weaker and the peak value is smaller. This will decrease the amplification factor.
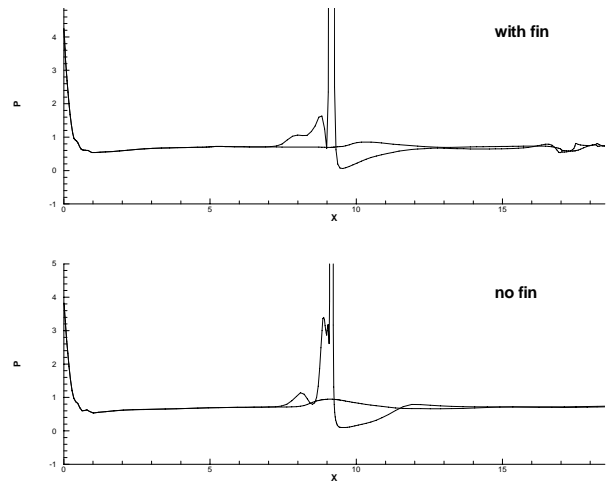

Fig. 6. Comparison of wall pressure at symmetrical plane

Table 2 shows the amplification factor Kf in case of with or without fins. Obviously, because of fins, the amplification factor is much lower than slender body.

Table 2: Effect of fins(H=6km，M=2.0，aoa=0)

	Fy (N)	Kf
With fin	-0.4370034E+04	0.7966236E+00
No fin	-0.5054395E+04	0.9211067E+00

6 Double jets

In fact, two or more jets will be used to change the lateral force value or its direction. Two kinds of double jets were calculated here. One is two jets with angle of 180 degrees (back to back) and the other is with 90 degrees.

Figure 7 and 8 show the Mach number and pressure distribution of dual jets with angle of 180 degree, angle of attack is 10 degree. The effect of angle of attack is apparent.

Table 3 compares the aero force of missile with and without lateral jets. The resultant force produced by lateral jets is 2381-3729＝-1348N

Table 3: Aero force of missile with/without lateral jets

	Fx (N)	Fy (N)
No jet	0.2625830E+04	0.3729046E+04
Dual jet	0.2659668E+04	0.2381162E+04
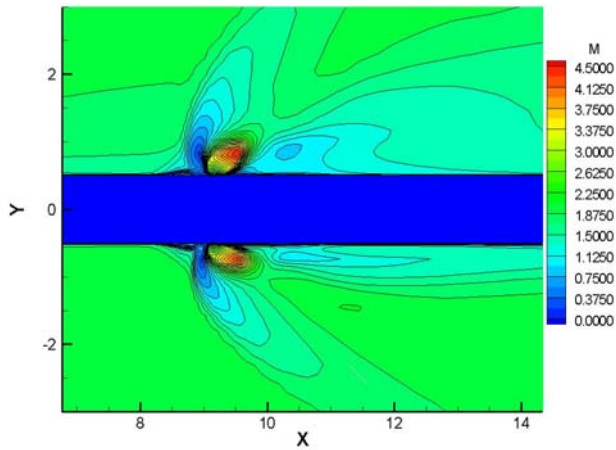
Fig. 7. Mach number distribution on symmetric plane with up and down injection
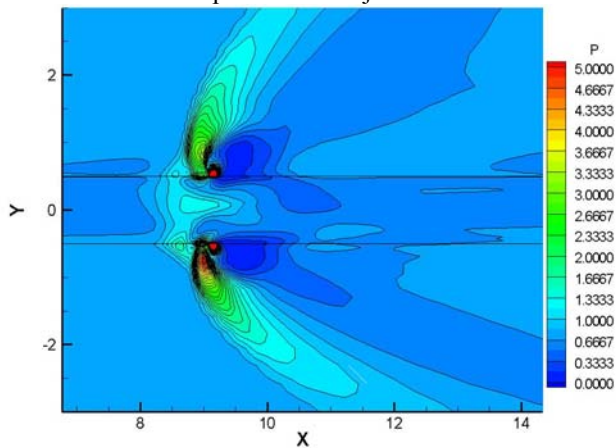
Fig.8. Pressure distribution on symmetric plane with up and down injection

Figure 9 gives the wall pressure distribution on the missile body with jets with 90 degrees. In calculation, angle of attack is zero. Because of the interaction of two jets, the final amplification factor is 1.12 for resultant force.
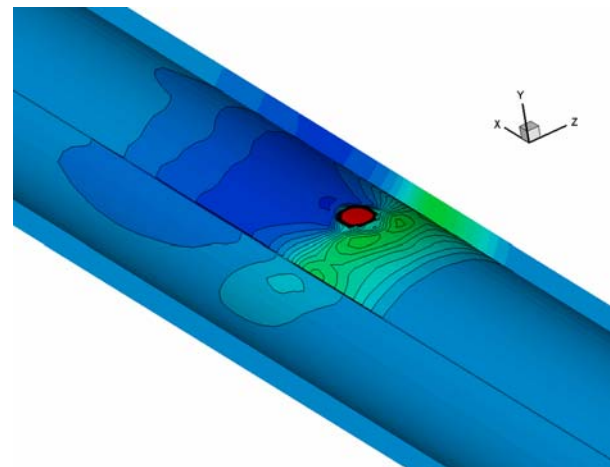
While in case of single injection under same condition, the amplification factor is about 0.8.
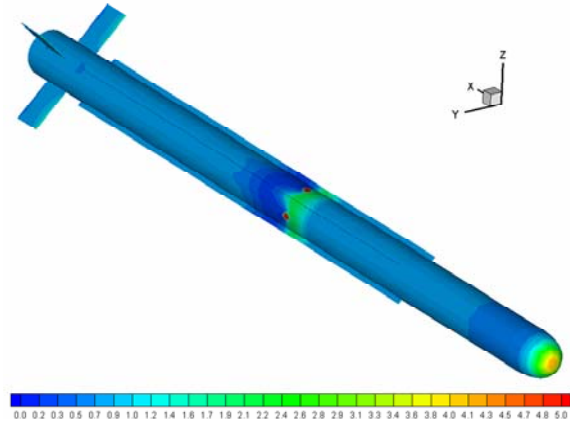
(a)
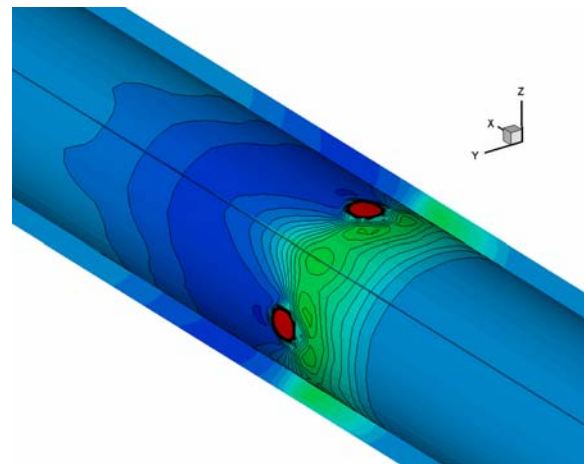
(b)

(c)

Fig. 9. Pressure distribution on the missile body surface with injections with 90 degrees

7 Conclusions

For air-to-air missile with lateral jet control, the flowfield is very complex because of the interaction. Moment and pressure at nozzle exit are the main factors that influence the lateral force. To keep same moment and pressure, the air jet and hot gas jet will give nearly same results.

Fins have great effect on the amplification factor of lateral jet because they disturb the wall pressure distribution.

The interaction of two jets will take effect on the resultant force. In case of zero angle of attack, the amplification factor will increase because of the interaction.

References

[1] Dechuan Sun, Chunbo Hu, Timin Cai**.** *Computation of supersonic turbulent flowfield with crossflow*. Applied Mathematics and Dynamics. Vol. 23, No. 1, 2002.

[2] Guang-Shan Jiang and Chi-Wang Shu. *Efficient Implementation of Weighted ENO Schemes*. Journal of Computational Physics 126, pp 202-228, 1996.

Copyright Statement